Purdue University
Purdue e-Pubs

Birck and NCN Publications | Birck Nanotechnology Center

7-29-2008

Highly ordered diamond and hybrid triangle-diamond patterns in porous anodic alumina thin films

Joshua T. Smith
Purdue University, jtsmith@purdue.edu

Qingling Hang
Purdue University, qhang@ecn.purdue.edu

Aaron D. Franklin
Purdue.University, aaron-franklin@purdue.edu

David B. Janes
Purdue University, janes@purdue.edu

Timothy D. Sands
Purdue University, tsands@purdue.edu

Follow this and additional works at: http://docs.lib.purdue.edu/nanopub

Smith, Joshua T.; Hang, Qingling; Franklin, Aaron D.; Janes, David B.; and Sands, Timothy D., "Highly ordered diamond and hybrid triangle-diamond patterns in porous anodic alumina thin films" (2008). *Birck and NCN Publications.* Paper 97.
http://docs.lib.purdue.edu/nanopub/97

This document has been made available through Purdue e-Pubs, a service of the Purdue University Libraries. Please contact epubs@purdue.edu for additional information.

Highly ordered diamond and hybrid triangle-diamond patterns in porous anodic alumina thin films

Joshua T. Smith,[1,2] Qingling Hang,[1,2] Aaron D. Franklin,[1,2] David B. Janes,[1,2] and Timothy D. Sands[1,2,3,a)]

[1]*Birck Nanotechnology Center, Purdue University, West Lafayette, Indiana 47907, USA*
[2]*School of Electrical and Computer Engineering, Purdue University, West Lafayette, Indiana 47907, USA*
[3]*School of Materials Engineering, Purdue University, West Lafayette, Indiana 47907, USA*

(Received 20 May 2008; accepted 21 June 2008; published online 29 July 2008)

Utilizing nonequilibrium formation kinetics in porous anodic alumina (PAA) thin films, diamond and hybrid triangle-diamond pore patterns are achieved. During anodization, the self-compensation abilities of PAA allow diamond-shaped pores to form by omitting certain sites in the surface prepatterning process. The effects of tessellation on cell formation in these arrangements yield elongated, regular, and partially compressed hexagonal cell structures leading to diamond, circular, and triangular pores, respectively. The diamond-shaped porous templates provide a low-cost option for the preparation of scalable nanostructures with diamond-shaped cross sections with utility in a range of nanoscale applications, including enhanced sensing and field emission. © *2008 American Institute of Physics*. [DOI: 10.1063/1.2957991]

Porous anodic alumina (PAA) has become a key templating material for the fabrication of many electronic, optoelectronic, and magnetic nanoscale devices and structures, including nanotubes,[1,2] nanowires,[3–5] two-dimensional (2D) photonic crystals,[6] and arrays of nanoparticles.[7,8] Interest in this material is centered on the ability of Al to self-assemble into porous nanochannel arrays of precise shape and dimension upon anodization, providing a low-cost, simple fabrication process for producing nanotemplates. Several reports have shown that by pretexturing the Al surface prior to anodization, highly ordered PAA templates can be fabricated as substrate-supported thin films.[9–11] Although the natural ordering of PAA takes the form of circular pores within hexagonally arranged cells,[12] square and triangular shaped pores and cells have been demonstrated by dimpling the Al surface using alternate tiling schemes.[13]

While nanostructures with diamond-shaped cross sections are promising candidates for several nanoscale applications, a method of creating templates with diamond-shaped pores has not yet been demonstrated. Nanoparticles with a controlled height, edge length, and tip sharpness are advantageous for optimizing sensitivity in localized surface plasmon resonance and surface-enhanced Raman spectroscopy.[14] A diamond geometry offers enhanced tip sharpness over triangular nanostructures fabricated to date that have been used for this purpose. This makes diamond nanostructures useful in the context of field-emission applications as well, offering a geometric advantage over triangular carbon nanotubes fabricated in PAA.[15]

Herein, we describe two patterns utilizing nonequilibrium tessellation arrangements that yield high-fidelity diamond and hybrid triangle-diamond pores in PAA thin films, providing a means of fabricating diamond nanostructures in a scalable template. Figure 1 provides a schematic representation of the layouts employed in the prepatterning process, with the patterned sites represented as blue dots. By maintaining a constant periodicity between each adjacent site while excluding certain locations (shown as smaller, red dots), the cell walls (dashed lines) surrounding the patterned locations can be expected to either elongate or compress, depending on the arrangement and orientation of the adjacent patterned and unpatterned regions. As will be discussed, the excluded locations will form smaller pores that play a crucial role in determining which of these cell types will be formed, and thus dictate the shape of the pores that appear at the patterned sites—diamond or triangle.

Patterns in the blue dot arrangements shown in Fig. 1 were transferred to Al surfaces via electron-beam lithography (EBL) on samples consisting of an e-beam evaporated Ti/Al stack (50 nm/500 nm) supported on Si substrates [Figs. 2(a) and 2(b)]. The exposed regions were wet etched for 90 s using Al Etchant—Type A (Transene Co.) to

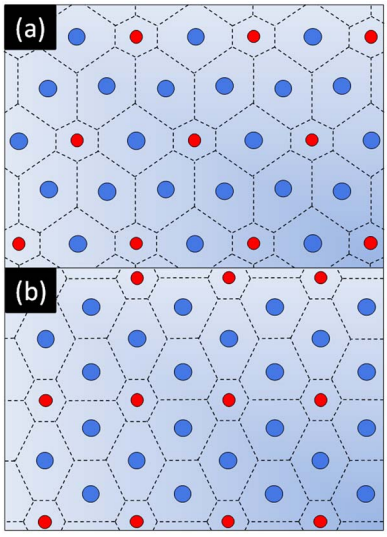

FIG. 1. (Color online) Schematic representations of the (a) diamond and (b) triangle-diamond pattern tiling schemes. Large, blue dots represent sites included in the prepatterning process and the smaller red dots indicate locations where compensated pores will appear. Dashed lines signify the location of cell wall formation.

a)Electronic mail: tsands@purdue.edu.

 © 2008 American Institute of Physics

Downloaded 29 Jul 2008 to 128.211.170.15. Redistribution subject to AIP license or copyright; see http://apl.aip.org/apl/copyright.jsp

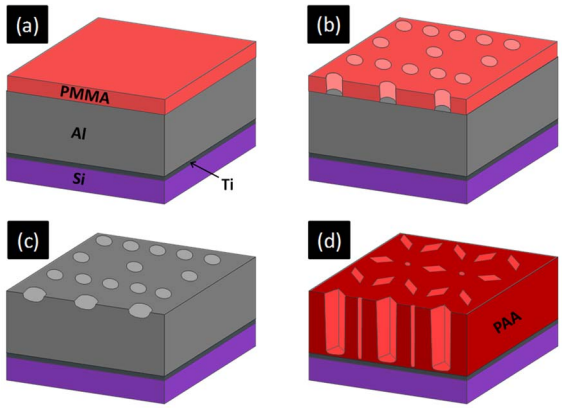

FIG. 2. (Color online) Process flow for the diamond template patterning scheme. (a) PMMA is applied to a Ti/Al stack supported on Si. (b) Pattern is defined using EBL and exposed regions are developed. (c) Concaves are isotropically etched in Al surface. PMMA is removed. (d) Sample is anodized to form diamond patterns.

a depth of ~70 nm [Fig. 2(c)] prior to polymethylmethacrylate (PMMA) removal. Atomic force microscopy measurements confirmed an Al surface roughness of <25 nm over 1 μm^2 areas in unpatterned regions, ensuring preferential pore growth in the etched locations. The samples were then anodized for 30 min at 120 V in 0.3M H_3PO_4 (5 °C) according to the well known linear voltage relationship (2.5 nm/V) to match the 300 nm periodicity of the etched locations,[16] producing uniform diamond patterns [Fig 2(d)]. While EBL is used here to pattern the Al surface, other surface patterning techniques that incorporate imprint molds can be applied to inexpensively replicate these patterns over large-scale areas ranging from several mm^2 to wafer-scale templates.[13,17]

The cell shapes achievable in PAA can be described in terms of Voronoi tessellation in the plane of the PAA surface.[18] Tessellating, or tiling, in this manner, results in cell geometries that completely fill the plane, where the cell walls form as the perpendicular bisectors of two adjacent nuclei.[13] Once formed, the nuclei, or etched pits in this case, act as initiation sites for pore growth by creating high localized electric fields during anodization that lead to higher currents and hence greater local dissociation of Al^{3+} ions.[19] Importantly, it is only the prepatterned arrangements and not the shape of the prepatterned features that determines the resulting pore and cell shapes formed.

The relationship between the pore patterns and resulting cell geometries can be understood in terms of a biaxial compressive stress in the plane of the film as it is oxidized during the anodization process. A volumetric expansion factor of ~1.2 has been shown to be the driving force for pore order in PAA.[20] During anodization, two distinct oxides are formed—the inner oxide that makes up the cell walls is composed of a dense pure alumina that is mechanically compressed by the competing expansion of adjacent pores, whereas the outer oxide surrounding each pore consists of an amorphous oxide.[21,22] Nielsch *et al.*[23] demonstrated that the ratio of the dense inner oxide thickness to that of the outer portion is a constant 0.2 ± 0.02 for well ordered, hexagonally arranged pores, regardless of the electrolyte type or applied potential. This translates to an outer oxide that is ~5× as thick as the inner cell walls—a property of PAA that is exploited to create our diamond and hybrid triangle-diamond templates.

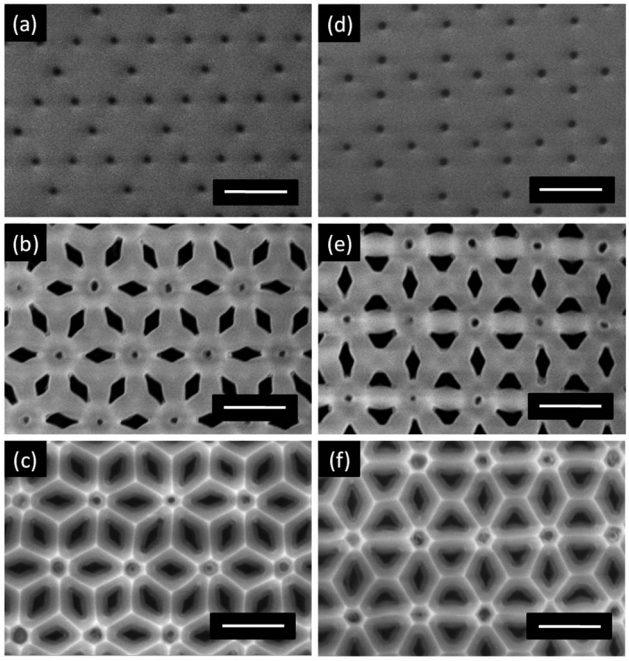

FIG. 3. FESEM images of diamond [(a)–(c)] and hybrid triangle-diamond [(d)–(f)] patterns. Postdeveloped PMMA surface of the diamond (a) and hybrid (d) prepatterning arrangements with 300 nm periodicity. Diamond (b) and hybrid triangle-diamond (e) porous templates following a single-step, 30 min anodization at 120 V in a 0.3M H_3PO_4 electrolyte (5 °C). Partially etched back alumina template showing the relative thicknesses of the inner (bright cell regions) and outer (semibright regions) oxides for the diamond (c) and hybrid (f) patterns. A SOG layer (darker region) covers the sidewalls surrounding the perimeter of the pore openings. All scale bars are 500 nm.

Figures 3(a)–3(c) show top view field-emission scanning electron microscope (FESEM) images illustrating the patterned PMMA, the resulting as-anodized PAA thin film, and a partially etched back PAA template for the diamond pattern. While the tiling of a 2D space by equilateral polygons is limited to triangles, squares, and regular hexagons for a completely patterned surface, elongated hexagonal cells are generated in the early stages of anodization when certain omitted locations are incorporated in the prepatterning process [Fig. 1]. A careful inspection of Figs. 3(a) and 3(b) reveals that every defined pore location is centered between two unpatterned pore sites in which smaller pores form, corresponding to the red dot locations in Fig. 1(a). The self-compensation abilities of PAA allow it to self-repair by forcing pore formation in locations not included in the prepatterning process when the omitted site is centered between six nearest neighbor patterned sites and the periodicity of the resulting pores is well matched to the anodization potential.[24] The elongated hexagonal cells that form as a result may be attributed to the competing stresses exerted by the faster forming patterned and slower developing compensated pore locations. In the diamond pattern arrangement, this stress imbalance results in smaller, hexagonal cells in the compensated locations and larger, elongated hexagonal cells forming at the patterned sites. In terms of pattern retention, it has been reported that self-repaired configurations are stable up to approximately 2 μm in hexagonally arranged patterns with a 200 nm interpore distance before becoming disordered due to the differ-

Downloaded 29 Jul 2008 to 128.211.170.15. Redistribution subject to AIP license or copyright; see http://apl.aip.org/apl/copyright.jsp

ence in growth rates.[24] According to the 10% porosity rule,[23] an aspect ratio of ~30 may then be expected, assuming that the relative growth rates of the compensated and diamond-shaped pores are similar to those previously reported. In the present work, cross-sectional images (not shown) of the diamond pores showed little variation in cell and pore structure throughout the 500 nm thick templates produced. Thus, by anodizing sufficiently thin, patterned Al films on a substrate, the integrity of the patterns is maintained.

To verify the relative cell geometries and oxide ratios in the templates created, a partial etch back procedure was employed. For this purpose, the pores were filled with a spin-on glass (SOG) material and cured at 425 °C for 1 h. The SOG top layer was then removed with a reactive-ion etch using a mixture of CF_4 and C_4F_8 until the material was etched back just inside the pores. Due to the somewhat isotropic nature of the dry etch process, a SOG coat remained on the sidewalls of the pores. With an etch barrier in place, the alumina template was partially etched back in a vertical fashion using a chromic acid mixture at 65 °C for 5 min, revealing the separate inner and outer oxide regions due to a slight disparity in their respective etch rates [Fig. 3(c)]. This provided a means of estimating the lateral thickness of both oxides using FESEM imaging.

The longer cell wall segments in this design coupled with the thicker outer oxide prevents the pore shape from being influenced by the smaller segments. The ratio of the inner to outer oxide shown is 0.23 ± 0.02, a number in good agreement with previous studies.[23] The outer oxide produces diamond-shaped pores in the elongated cells since it is thick enough in the regions adjacent to the longer cell wall segments to close the tips of the diamond shape before the oxide extending from the smaller segments can to contribute to the pore geometry. With small hexagonal cells surrounding compensated pore locations, the cumulative pore pattern is comprised of diamond-shaped pores concentrically centered about small circular pores in a repeating petal-like arrangement [Fig 3(b)].

A more complex pattern was created that resulted in templates with both triangle- and diamond-shaped pores in a single periodic array, further illustrating the formation mechanisms that allow nonequilibrium pore shapes to be realized [Fig. 3(d)]. Upon anodization, the cell walls form into elongated, partially compressed, and regular hexagonal shapes, leading to diamond, triangle, and small circular pores, respectively [Fig. 3(e)]. The etch procedures employed for the diamond pattern were applied here as well to aid in the analysis of cell wall and pore formation [Fig. 3(f)]. In a partially compressed hexagonal cell, a triangular-shaped pore forms since the outer oxide is sufficiently thick to suppress the contributions of the three shorter cell segments. Notably, the longest of these segments does appear to have a flattening effect on the apex the triangle pores—an observation consistent with the concept that the larger the segment, the greater its effect will be on the resulting pore shape.

In conclusion, we have demonstrated how nonequilibrium formation conditions in PAA can be exploited to create PAA thin films with diamond and hybrid triangle-diamond pore shapes by appropriately incorporating pore omission arrangements in the surface prepatterning process to alter the cell shapes produced. A sharp-featured diamond and triangular pore growth was attributed to the thick outer oxide within the cells suppressing or eliminating the influence of the smaller cell segments on the geometry of the pore shapes produced. The patterns allow high-fidelity, diamond-shaped pores to be fabricated in a scalable template. These templates are candidates for the fabrication of densely packed nanostructures for a variety of nanoscale applications.

We acknowledge support from the Birck Nanotechnology Center. J.T.S. and A.D.F. also recognize support from National Science Foundation (NSF) Graduate Research Fellowships.

[1] M. R. Maschmann, A. D. Franklin, A. Scott, D. B. Janes, T. D. Sands, and T. S. Fisher, Nano Lett. **6**, 2712 (2006).
[2] M. Lahav, E. A. Weiss, Q. Xu, and G. M. Whitesides, Nano Lett. **6**, 2166 (2006).
[3] O. Rabin, P. R. Herz, Y. M. Lin, A. I. Akinwande, S. B. Cronin, and M. S. Dresselhaus, Adv. Funct. Mater. **13**, 631 (2003).
[4] A. D. Franklin, M. R. Maschmann, M. DaSilva, D. B. Janes, T. S. Fisher, and T. D. Sands, J. Vac. Sci. Technol. B **25**, 343 (2007).
[5] S. Zhao, L. Clime, K. Chan, F. Normandin, H. Roberge, A. Yelon, R. W. Cochrane, and T. Veres, J. Nanosci. Nanotechnol. **7**, 381 (2007).
[6] H. Masuda, M. Yamada, F. Matsumoto, S. Yokoyama, S. Mashiko, M. Nakao, and K. Nishio, Adv. Mater. (Weinheim, Ger.) **18**, 213 (2006).
[7] H. Masuda, K. Yasui, and K. Nishio, Adv. Mater. (Weinheim, Ger.) **12**, 1031 (2000).
[8] C. Kim, T. Loedding, S. Jang, H. Zeng, Z. Li, Y. Sui, and D. J. Sellmyer, Appl. Phys. Lett. **91**, 172508 (2007).
[9] Z. Sun and H. K. Kim, Appl. Phys. Lett. **81**, 3458 (2002).
[10] R. Krishnan, H. Q. Nguyen, C. V. Thompson, W. K. Choi, and Y. L. Foo, Nanotechnology **16**, 841 (2005).
[11] Y. Lei, W. Cai, and G. Wilde, Prog. Mater. Sci. **52**, 465 (2007).
[12] F. Keller, M. S. Hunter, and D. L. Robinson, J. Electrochem. Soc. **100**, 411 (1953).
[13] H. Masuda, H. Asoh, M. Watanabe, K. Nishio, M. Nakao, and T. Tamamura, Adv. Mater. (Weinheim, Ger.) **13**, 189 (2001).
[14] L. J. Sherry, R. Jin, C. A. Mirkin, G. C. Schatz, and R. P. Van Duyne, Nano Lett. **6**, 2060 (2006).
[15] T. Yanagishita, M. Sasaki, K. Nishio, and H. Masuda, Adv. Mater. (Weinheim, Ger.) **16**, 429 (2004).
[16] K. Ebihara, H. Takahashi, and M. Nagayama, J. Met. Finish. Soc. Jpn. **34**, 548 (1983).
[17] W. Lee, R. Ji, C. A. Ross, U. Gösele, and K. Nielsch, Small **2**, 978 (2006).
[18] J. Broughton and G. A. Davies, J. Membr. Sci. **106**, 89 (1995).
[19] O. Jessensky, F. Müller, and U. Gösele, Appl. Phys. Lett. **72**, 1173 (1998).
[20] A. P. Li, F. Müller, and U. Gösele, Electrochem. Solid-State Lett. **3**, 131 (2000).
[21] G. E. Thompson and G. C. Wood, *Anodic Films on Aluminum, in Treatise on Materials Science and Techology*, edited by J. Scully, (Academic, New York, 1983) Vol. 23, Chap 5, p. 205.
[22] J. Choi, Y. Luo, R. B. Wehrspohn, R. Hillebrand, J. Schilling, and U. Gösele, J. Appl. Phys. **94**, 4757 (2003).
[23] K. Nielsch, J. Choi, K. Schwirn, R. B. Wehrspohn, and U. Gösele, Nano Lett. **2**, 677 (2002).
[24] H. Masuda, M. Yotsuya, M. Asano, and K. Nishio, Appl. Phys. Lett. **78**, 826 (2001).

Downloaded 29 Jul 2008 to 128.211.170.15. Redistribution subject to AIP license or copyright; see http://apl.aip.org/apl/copyright.jsp